Endohedral Tin Cages

DOI: 10.1002/anie.200603226

Endohedral Stannaspherenes $M@Sn_{12}^-$: A Rich Class of Stable Molecular Cage Clusters**

Li-Feng Cui, Xin Huang, Lei-Ming Wang, Jun Li, and Lai-Sheng Wang**

Since the discovery and bulk synthesis of fullerenes,[1,2] there have been great expectations in cluster science to uncover other stable atomic clusters that may be used as building blocks for cluster-assembled nanomaterials. The heavy congeners of carbon in Group 14 were not known to form fullerene-like empty cage structures until very recently, when it was discovered serendipitously that a 12-atom Sn cluster forms a highly stable empty cage (Sn_{12}^{2-}, stannaspherene)[3] with a large inner diameter (6.1 Å) that is only slightly smaller than that of C_{60}. Although polyhedral cages are common in inorganic compounds,[4,5] empty cage clusters with large internal volumes are rare.[6,7] Stannaspherene can be viewed as a real inorganic analogue of the fullerenes because of its spherical π bonding,[3] which is similar to that in the $B_{12}H_{12}^{2-}$ cage molecule.[8,9] Several metal-encapsulated cage clusters of heavy Group 14 elements are known,[10–22] but the metal encapsulation was thought to be essential to stabilize the cage structure. Here, we report that stannaspherene can trap an atom from any of the transition metals or the f-block elements to form a large class of new endohedral cage clusters. We have produced a set of $M@Sn_{12}^-$ cages (M = Ti, V, Cr, Fe, Co, Ni, Cu, Y, Nb, Gd, Hf, Ta, Pt, Au) by laser vaporization and characterized them by photoelectron spectroscopy. Both experimental and theoretical evidence shows that these clusters have perfect or pseudo-icosahedral symmetry, with the central atom inducing very little distortion in the Sn_{12}^{2-} cage. Since the central atom in $M@Sn_{12}^-$ maintains its quasi-atomic nature, as in the endohedral fullerenes,[23,24] the clusters are a rich class of potential building blocks for new materials with tunable electronic, magnetic, or chemical properties.

The experiment was carried out on a magnetic-bottle photoelectron spectroscopy apparatus equipped with a laser vaporization cluster source (see Experimental Section).[25] Figure 1 shows the 193-nm photoelectron spectra of Sn_{12}^- doped with 3d transition metals and selected 4d and 5d dopants. (More spectra with other dopants, including rare-earth elements, are given in the Supporting Information .) All spectra are well resolved and show numerous distinct electronic transitions. In general, the spectra of $M@Sn_{12}^-$ become more complicated as one moves from Cu to the left of the transition series due to the open d shell and the relative orbital-energy variation of the 3d electrons, which are core-like in Cu but become frontier levels in the early transition metals. Remarkably, there is a characteristic doublet feature near 5 eV (labeled g_u in Figure 1), which is present in all spectra, with little variation between the different $M@Sn_{12}^-$ species.

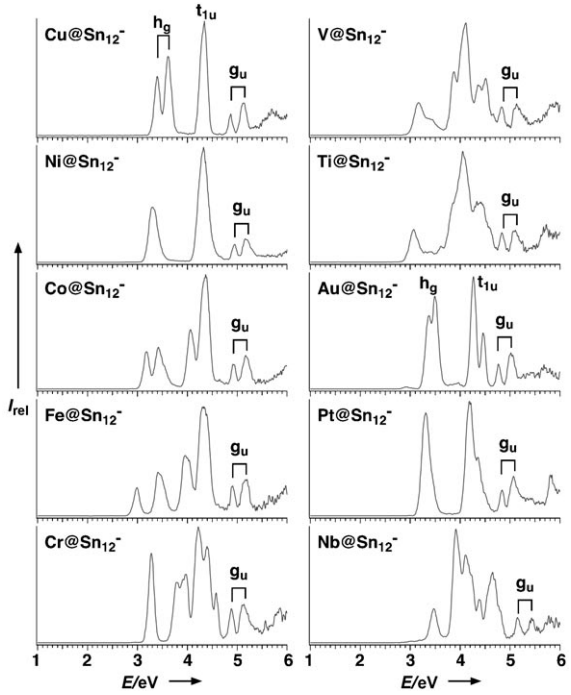

Figure 1. Photoelectron spectra of selected $M@Sn_{12}^-$ at 193 nm (6.424 eV).

[*] Dr. J. Li
W. R. Wiley Environmental Molecular Sciences Laboratory
Pacific Northwest National Laboratory, MS K1-96
P.O. Box 999, Richland, WA 99352 (USA)
Fax: (+1) 509-376-0420
E-mail: jun.li@pnl.gov
L.-F. Cui, Dr. X. Huang, L.-M. Wang, Prof. Dr. L.-S. Wang
Department of Physics, Washington State University
2710 University Drive, Richland, WA 99354 (USA)
and
Chemical Sciences Division
Pacific Northwest National Laboratory, MS K8-88
P.O. Box 999, Richland, WA 99352 (USA)
Fax: (+1) 509-376-6066
E-mail: ls.wang@pnl.gov

[**] This work was supported by the US National Science Foundation (DMR-0503383) and performed at the W. R. Wiley Environmental Molecular Sciences Laboratory (EMSL), a national scientific user facility sponsored by the DOE's Office of Biological and Environmental Research and located at the Pacific Northwest National Laboratory (PNNL), which is operated for the DOE by Battelle. The calculations were performed partly at the Molecular Science Computing Facility (MSCF) located at EMSL, PNNL.

Supporting Information for this article is available on the WWW under http://www.angewandte.org or from the author.

Our previous study has shown that the stannaspherene Sn_{12}^{2-} possesses an inner diameter of 6.1 Å,[3] which is large enough to trap any transition metal, f-block element, or certain main-group elements. The doublet feature near 5 eV in all $M@Sn_{12}^-$ clusters bears considerable resemblance to similar spectral features primarily derived from the on-sphere g_u σ orbitals in stannaspherene (Figure 3), which suggests that all $M@Sn_{12}^-$ clusters possess similar structures and that the Sn_{12} cage is intact in $M@Sn_{12}^-$.

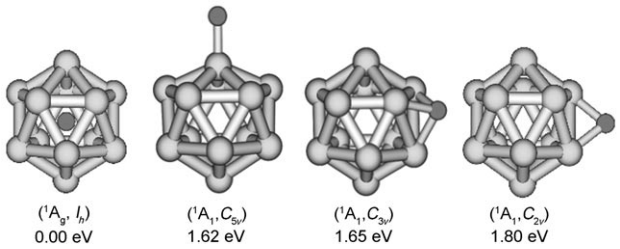

Figure 2. Optimized structure of the global minimum endohedral $Cu@Sn_{12}^-$ cluster along with several exohedral $CuSn_{12}^-$ clusters and their relative energies. Cu dark gray, Sn light gray.

To confirm the endohedral nature of the $M@Sn_{12}^-$ cages and understand their electronic structure, we performed extensive theoretical calculations (see Experimental Section). Here we focus on the $CuSn_{12}^-$ system (Figure 2). Our theoretical results indicate that endohedral $Cu@Sn_{12}^-$ is indeed overwhelmingly more stable than any of the exohedral isomers. The calculated adiabatic and vertical detachment energies and simulated photoelectron spectrum of the endohedral $Cu@Sn_{12}^-$ with spin–orbit coupling are in excellent agreement with the experimental data (Figure S2), thus confirming unequivocally its stability and structure.

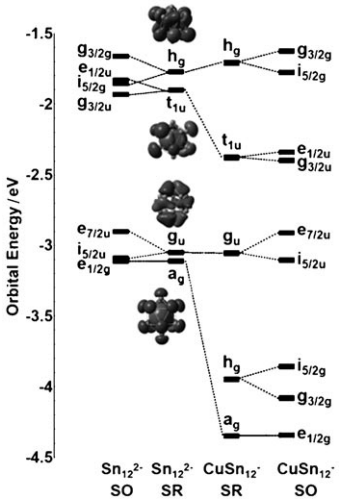

Figure 3. Correlation diagram between the scalar-relativistic (SR) valence levels of Sn_{12}^{2-} and $Cu@Sn_{12}^-$ and their spin–orbit (SO)-split levels. The SR molecular orbital contour surfaces of Sn_{12}^{2-} are also shown. The lower h_g orbital in $Cu@Sn_{12}^-$ is the Cu 3d shell.

$Cu@Sn_{12}^-$ is a perfect icosahedral cluster (I_h; Figure 2) with a Sn–Sn distance (3.21 Å) very close to that in stannaspherene (3.19 Å), which suggests only moderate interactions between the central Cu atom and the Sn_{12} cage. The Cu–Sn distance (3.05 Å) in $Cu@Sn_{12}^-$ is considerably longer than the Cu–Sn distance (2.6 Å) in diatomic CuSn,[26] which is consistent with relatively weak covalent interactions between Cu and the Sn_{12} cage in $Cu@Sn_{12}^-$. In fact, $Cu@Sn_{12}^-$ can be described as a Cu^+ ion trapped inside stannaspherene ($[Cu^+@Sn_{12}^{2-}]$), similar to the charge-transfer complexes formed in endohedral fullerenes.[23,24,27]

Figure 3 compares the scalar-relativistic (SR) and spin–orbit (SO)-coupled energy levels of the valence molecular orbitals (MO) of $Cu@Sn_{12}^-$ and those of stannaspherene. As we showed previously, stannaspherene is bonded by the Sn 5p electrons only, which transform into h_g, t_{1u}, g_u, and a_g valence MOs (Figure 3), whereas the Sn 5s electrons are mainly nonbonding lone pairs. Upon insertion of Cu^+ into Sn_{12}^{2-}, the radial bonding MOs (a_g and t_{1u}) are stabilized because they are symmetry-allowed to interact with the d orbitals of the dopant, whereas the purely tangential g_u MO is not affected at all because of symmetry restrictions. The h_g highest occupied molecular orbital (HOMO), which has a small amount of mixing from the radial orbitals, is slightly destabilized. The filled $3d^{10}$ shell of the Cu^+ ion transforms into an h_g orbital in $Cu@Sn_{12}^-$ whilst maintaining its fivefold degeneracy. When SO coupling is taken into account, each degenerate orbital is split into two levels. The SO coupling in the corresponding MOs in $Cu@Sn_{12}^-$ and Sn_{12}^{2-} is very similar (Figure 3). The SO-split MO pattern of $Cu@Sn_{12}^-$ is in excellent agreement with the observed spectral pattern, as can be seen in the spectrum of $Cu@Sn_{12}^-$ (Figure 1). The Cu 3d levels and the a_g orbitals have too high binding energies to be ionized at the photon energy used. The SO splittings in the h_g HOMO and the g_u orbitals are large enough to be clearly resolved experimentally.

The spectrum of $Au@Sn_{12}^-$ is almost identical to that of $Cu@Sn_{12}^-$ except that the SO splitting in the t_{1u} orbital is enhanced in $Au@Sn_{12}^-$, which is also borne out by our calculations, thus confirming the endohedral nature of-ctjl;$Au@Sn_{12}^-$. The first adiabatic detachment energy (ADE) and vertical detachment energy (VDE) of $Cu@Sn_{12}^-$ and $Au@Sn_{12}^-$ are identical within our experimental uncertainties (see Supporting Information).

Although the $Cu@Sn_{12}^-$ cluster has perfect icosahedral symmetry, our calculations show that the other endohedral $M@Sn_{12}^-$ clusters with open d shells on the central dopant, except $Cr@Sn_{12}^-$ (see Supporting Information), have slightly distorted structures, owing to the Jahn–Teller effect. However, these structural distortions are very small and the actual cage structures of all $M@Sn_{12}^-$ clusters are very close to the ideal I_h symmetry. The nearly identical doublet features near 5 eV in all spectra of the $M@Sn_{12}^-$ clusters are due to the same g_u orbitals (Figure 1), which are purely on-sphere σ orbitals (Figure 3) and are not expected to be affected by the central atom. This spectral characteristic provides a fingerprint for the endohedral cage structures for all $M@Sn_{12}^-$ clusters and reflects the robustness of the stannaspherene cage. The more complicated spectral features in the lower binding energy

range in the $M@Sn_{12}^-$ clusters with open d shells are as expected.

For the late transition metal dopants (M = Ni, Fe, Co), our calculations show that the 3d electrons are still significantly lower in energy and cannot be detached at 193 nm. The extra spectral features in $Co@Sn_{12}^-$ and $Fe@Sn_{12}^-$ are likely due to spin polarization of the h_g HOMO and the t_{1u} orbitals. For the early transition metal dopants (Cr, V, Ti), the 3d electrons have similar binding energies to the Sn-derived frontier h_g and t_{1u} orbitals, which results in much more complex spectral patterns due to direct detachment from the 3d valence levels in the low binding energy region (Figure 1).

The 4d and 5d dopants behave similarly to the 3d dopants, which results in similar photoelectron spectra for the corresponding endohedral stannaspherenes. Our photoelectron spectra suggest that the rare-earth atoms also form endohedral stannaspherenes, as indicated by the g_u doublet spectral fingerprint in the spectra of $Y@Sn_{12}^-$ and $Gd@Sn_{12}^-$ (see Supporting Information) and confirmed subsequently by theoretical calculations.

All $M@Sn_{12}^-$ anions can be described as $[M^+@Sn_{12}^{2-}]$, whereas the neutral endohedral stannaspherenes $M@Sn_{12}$ can be described as $[M^{2+}@Sn_{12}^{2-}]$. For the 3d dopants, all endohedral stannaspherenes are magnetic with high spins resulting from the 3d-electron configurations of the transi-c-tjl;tion metals, which range from $3d^2$ in $[Ti^{2+}@Sn_{12}^{2-}]$ to $3d^8$ in $[Ni^{2+}@Sn_{12}^{2-}]$. Thus, a new class of cage clusters with tunable magnetic and optical properties is accessible.[28] In contrast to the encapsulated Si or Ge clusters, where the dopants are critical to stabilize the cage structures,[10–17] the stability of $M@Sn_{12}$ derives from the intrinsic stability of stannaspherene itself, much like the endohedral fullerenes. Our study indicates that all transition metal or f-block atoms can be trapped inside stannaspherene. This is an important advantage with respect to the endohedral fullerenes, which can only trap alkali, alkaline earth, or rare-earth atoms; the chemically more interesting transition metal atoms do not form endohedral fullerenes.[27]

Ni- or Pt-encapsulated Pb_{12} icosahedral clusters similar to $Ni@Sn_{12}^-$ or $Pt@Sn_{12}^-$ have been synthesized in solution-ctjl;and characterized in the bulk.[18,20,22] Even though the doped Ni or Pt atom was thought to be essential for the cage compounds, we have evidence that Pb_{12}^{2-} is also a highly stable empty cage cluster (plumbaspherene)[7] similar to Sn_{12}^{2-}, both of which are isoelectronic with the well-known borane cage molecule $B_{12}H_{12}^{2-}$.[8,9] Hence, the previously observed $Pt@Pb_{12}^{2-}$ and $Ni@Pb_{12}^{2-}$ anions, as well as the $Al@Pb_{12}^+$ cation ($[Al^{3+}@Pb_{12}^{2-}]$),[19] should belong to a whole family of endohedral plumbaspherenes that are similar to the endohedral stannaspherenes. Icosahedral $M@Au_{12}$-type cage clusters have also been predicted[29] and observed experimentally.[30] However, similar to the metal-encapsulated Si or Ge clusters,[10–17] the dopant is critical for the cage structure of $M@Au_{12}$ because bare Au_{12} does not possess a cage structure.[31] If flexible, bulk synthetic methods can be found for this vast number of endohedral stannaspherenes, it may be possible to create novel cluster-assembled materials with continuously tunable electronic, magnetic, or optical properties across the entire transition series or the f block.

Experimental Section

Cluster generation, mass selection, and photoelectron spectroscopy: All experiments were carried out on a magnetic-bottle photoelectron spectroscopy apparatus equipped with a laser vaporization cluster source, details of which have been described previously.[25] The targets were prepared by pressing a mixed powder of tin with the desired dopant (M = Ti, V, Cr, Fe, Co, Ni, Cu, Y, Nb, Gd, Hf, Ta, Pt, Au). The pressed Sn/M disk target was vaporized by the second harmonic output (532 nm) of a Nd:YAG laser. The laser-induced plasma was entrained in a high pressure helium carrier gas in which the vaporized Sn and M atoms nucleate to form pure Sn clusters and Sn clusters doped with the desired impurity atom. It was important to adjust the M/Sn ratio in the target so that only one or two dopant atoms were incorporated into the Sn clusters. We found that targets prepared with less than 10% dopant by atom yielded mainly clusters with only one doped atom (MSn_x^-), along with pure Sn_x^- clusters.

Negatively charged clusters from the laser vaporization source were extracted from the cluster beam and subjected to a time-of-flight mass analysis. The clusters of interest (MSn_{12}^-) were mass-selected and decelerated before crossing with a laser beam for photodetachment. Photoemitted electrons were analyzed by a magnetic-bottle time-of-flight electron analyzer calibrated against the known spectrum of Pt^-. The electron energy resolution of the magnetic-bottle spectrometer was $\Delta E/E \approx 2.5\%$ (i.e., 25 meV) for 1 eV electrons. Because of the broad isotopic distribution of Sn, the mass gate was carefully set to minimize contamination of the selected MSn_{12}^- peaks from pure Sn_x^- clusters. Negligible contamination was achieved for all PES spectra reported in the current work.

Calculations: All structures were optimized using density functional theory at the B3LYP level, and frequency calculations were performed to confirm that the calculated structures were minima.[32,33] The Stuttgart small-core relativistic effective core potentials and basis sets were used to describe Sn, Ti, V, Cr, Fe, Co, Ni, Cu, and K, with polarization and diffuse functions added for Sn ($\zeta(d) = 0.183$, $\zeta(p) = 0.0231$).[34] The calculations were accomplished using the NWChem 4.7 program.[35]

Because of the importance of spin–orbit coupling effects in the Sn clusters, we also performed two-component relativistic DFT calculations using the zero-order regular approximation (ZORA)[36] implemented in the Amsterdam Density Functional (ADF) code.[37] These calculations used the PW91 exchange-correlation functional[38] and the TZ2P Slater basis sets with the frozen-core approximation.[37] The electron detachment spectra (see Supporting Information) were simulated by fitting the calculated spin–orbit energies with Gaussian functions, and the intensities were not explicitly computed.

Received: August 8, 2006
Revised: September 21, 2006
Published online: December 5, 2006

Keywords: cage compounds · cluster compounds · density functional calculations · photoelectron spectroscopy · tin

[1] H. W. Kroto, J. R. Heath, S. C. O'Brien, R. F. Curl, R. E. Smalley, *Nature* **1985**, *318*, 162–163.
[2] W. Krätschmer, L. D. Lamb, K. Fostiropoulos, D. R. Huffman, *Nature* **1990**, *347*, 354–358.
[3] L. F. Cui, X. Huang, L. M. Wang, D. Y. Zubarev, A. I. Boldyrev, J. Li, L. S. Wang, *J. Am. Chem. Soc.* **2006**, *128*, 8390–8391.
[4] J. D. Corbett, *Angew. Chem.* **2000**, *112*, 682–704; *Angew. Chem. Int. Ed.* **2000**, *39*, 670–690.
[5] S. Alvarez, *Dalton Trans.* **2005**, 2209–2233.
[6] J. Bai, A. V. Virovets, M. Scheer, *Science* **2003**, *300*, 781–783.
[7] We have found recently that Pb_{12}^{2-} is also a stable icosahedral cage cluster (L. F. Cui, X. Huang, L. M. Wang, J. Li, L. S. Wang,

J. Phys. Chem. A **2006**, *110*, 10169 – 10172), and an empty Pb_{10}^{2-} cage cluster has been characterized recently (A. Spiekermann, S. D. Hoffmann, T. F. Fässler, *Angew. Chem.* **2006**, *118*, 3538 – 3541; *Angew. Chem. Int. Ed.* **2006**, *45*, 3459 – 3462). Although gold clusters have been proposed to form cage clusters (M. P. Johansson, D. Sundholm, J. Vaara, *Angew. Chem.* **2004**, *116*, 2732 – 2735; *Angew. Chem. Int. Ed.* **2004**, *43*, 2678 – 2681) experimental evidence of gold cage clusters in the size range between Au_{16}^- and Au_{18}^- has been reported only very recently (S. Bulusu, X. Li, L. S. Wang, X. C. Zeng, *Proc. Natl. Acad. Sci. USA* **2006**, *103*, 8326 – 8330).

[8] H. C. Longuet-Higgins, M. de V. Roberts, *Proc. R. Soc. London Ser. A* **1955**, *230*, 110 – 119.

[9] A. R. Pitochelli, M. F. Hawthorne, *J. Am. Chem. Soc.* **1960**, *82*, 3228 – 3229.

[10] S. M. Beck, *J. Chem. Phys.* **1987**, *87*, 4233 – 4234.

[11] H. Hiura, T. Miyazaki, T. Kanayama, *Phys. Rev. Lett.* **2001**, *86*, 1733 – 1736.

[12] V. Kumar, Y. Kawazoe, *Phys. Rev. Lett.* **2001**, *87*, 045503.

[13] S. N. Khanna, B. K. Rao, P. Jena, *Phys. Rev. Lett.* **2002**, *89*, 016803.

[14] K. Koyasu, M. Akutsu, M. Mitsui, A. Nakajima, *J. Am. Chem. Soc.* **2005**, *127*, 4998 – 4999.

[15] V. Kumar, Y. Kawazoe, *Appl. Phys. Lett.* **2002**, *80*, 859 – 861.

[16] C. Schrodt, F. Weigend, R. Ahlrichs, *Z. Anorg. Allg. Chem.* **2002**, *628*, 2478 – 2482.

[17] V. Kumar, A. K. Singh, Y. Kawazoe, *Nano Lett.* **2004**, *4*, 677 – 681.

[18] E. N. Esenturk, J. Fettinger, Y. F. Lam, B. Eichhorn, *Angew. Chem.* **2004**, *116*, 2184 – 2186; *Angew. Chem. Int. Ed.* **2004**, *43*, 2132 – 2134.

[19] S. Neukermans, E. Janssens, Z. F. Chen, R. E. Silverans, P. von R. Schleyer, P. Lievens, *Phys. Rev. Lett.* **2004**, *92*, 163401.

[20] E. N. Esenturk, J. Fettinger, B. Eichhorn, *Chem. Commun.* **2005**, 247 – 249.

[21] G. A. Breaux, D. A. Hillman, C. M. Neal, M. F. Jarrold, *J. Phys. Chem. A* **2005**, *109*, 8755 – 8759.

[22] E. N. Esenturk, J. Fettinger, B. Eichhorn, *J. Am. Chem. Soc.* **2006**, *128*, 9178 – 9186.

[23] Y. Chai, T. Guo, C. Jin, R. E. Haufler, L. P. F. Chibante, J. Fure, L. Wang, J. M. Alford, R. E. Smalley, *J. Phys. Chem.* **1991**, *95*, 7564 – 7568.

[24] D. S. Bethune, R. D. Johnson, J. R. Salem, M. S. de Vries, C. S. Yannoni, *Nature* **1993**, *366*, 123 – 128.

[25] L. S. Wang, H. Wu, *Advances in Metal and Semiconductor Clusters. IV. Cluster Materials* (Ed.: M. A. Duncan), JAI Press, Greenwich, **1998**, pp. 299 – 343.

[26] W. Plass, H. Stoll, H. Preuss, A. Savin, *J. Mol. Struct. (Theochem)* **1995**, *339*, 67 – 81.

[27] T. Guo, R. E. Smalley, G. E. Scuseria, *J. Chem. Phys.* **1993**, *99*, 352 – 359.

[28] The $M@Sn_{12}$ endohedral clusters with open d shells may be more reactive and may exist in different charge states if synthesized in bulk.

[29] P. Pyykkö, N. Runeberg, *Angew. Chem.* **2002**, *114*, 2278 – 2280; *Angew. Chem. Int. Ed.* **2002**, *41*, 2174 – 2176.

[30] X. Li, B. Kiran, J. Li, H. J. Zhai, L. S. Wang, *Angew. Chem.* **2002**, *114*, 4980 – 4983; *Angew. Chem. Int. Ed.* **2002**, *41*, 4786 – 4789.

[31] F. Furche, R. Ahlrichs, P. Weis, C. Jacob, S. Gilb, T. Bierweiler, M. M. Kappes, *J. Chem. Phys.* **2002**, *117*, 6982 – 6990.

[32] A. D. Becke, *J. Chem. Phys.* **1993**, *98*, 5648 – 5652.

[33] C. Lee, W. Yang, R. G. Parr, *Phys. Rev. B* **1988**, *37*, 785 – 789.

[34] A. Bergner, M. Dolg, W. Kuechle, H. Stoll, H. Preuss, *Mol. Phys.* **1993**, *80*, 1431 – 1441.

[35] "NWChem, A Computational Chemistry Package for Parallel Computers, Version 4.7" (2005), Pacific Northwest National Laboratory, Richland, Washington 99352-0999, USA.

[36] E. van Lenthe, E. J. Baerends, J. G. Snijders, *J. Chem. Phys.* **1993**, *99*, 4597 – 4610.

[37] ADF 2005.01, SCM, Theoretical Chemistry, Vrije Universiteit, Amsterdam, The Netherlands (http://www.scm.com).

[38] J. P. Perdew, Y. Wang, *Phys. Rev. B* **1992**, *45*, 13244 – 13249.

